ALP-1996-109

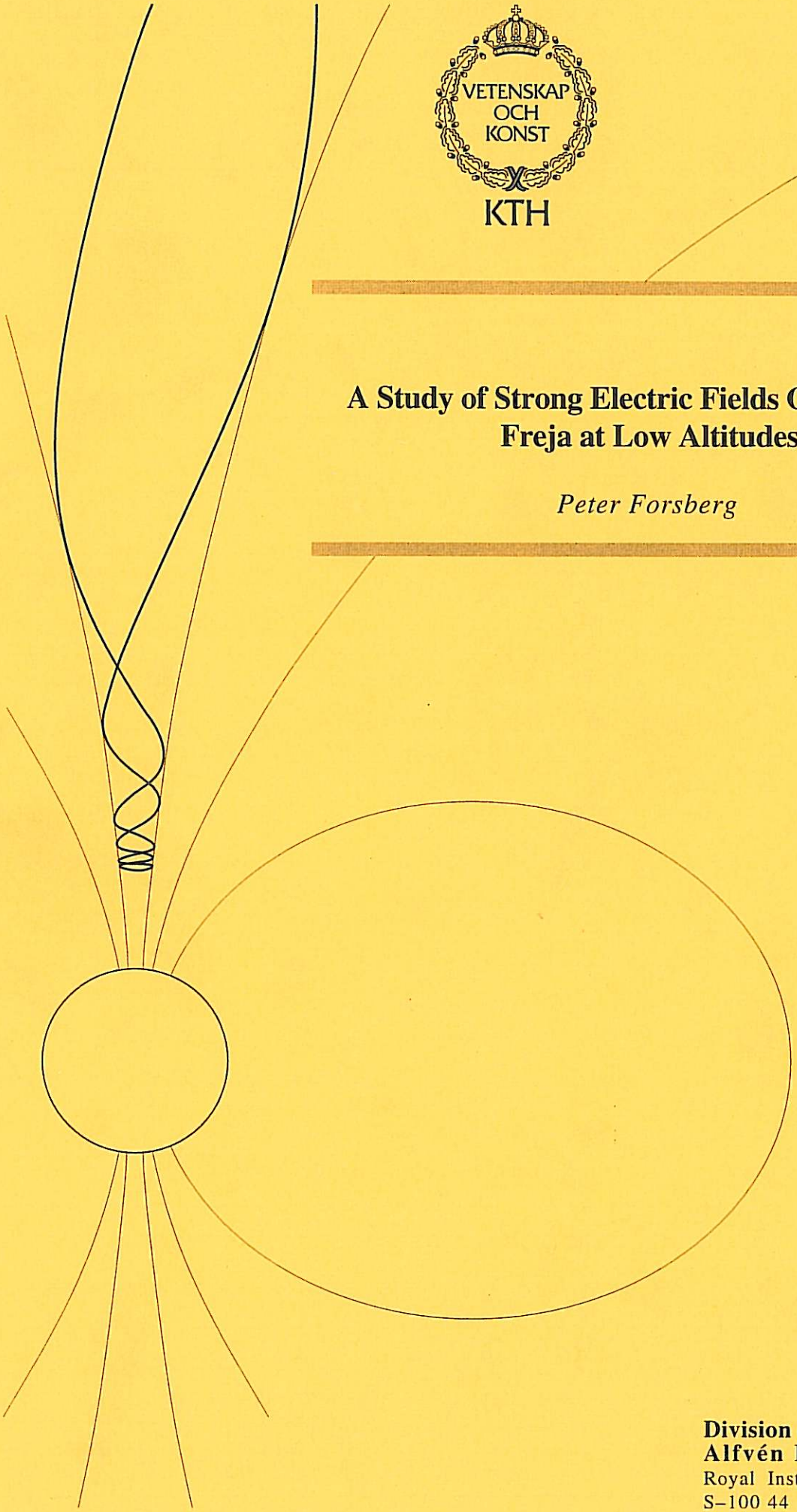

A Study of Strong Electric Fields Observed by Freja at Low Altitudes

Peter Forsberg

Division of Plasma Physics
Alfvén Laboratory
Royal Institute of Technology
S–100 44 Stockholm, Sweden

Contents

Abstract

The aurora is a phenomenon that has fascinated people at all times. The aim of this study is to investigate one of the many features connected to the aurora, namely the auroral electric field and related potential structures. For that purpose the electric field measured by the Freja satellite at altitudes around 800 km has been investigated. This is the continuation of a previous investigation [Marklund *et al.*, 1994, 1995ab; Karlsson and Marklund, 1996] of Freja data from altitudes around 1700 km. The underlying physics of the aurora, as well as the physical situation in the vicinity of the Earth, is presented, as is some work of relevance to this study, made by previous investigators. The main results from the present and the previous Freja investigations are as follows: Very intense electric fields occur occasionally in the auroral regions at altitudes down to below 650 km. Some of the strongest fields show a divergent structure. In the previous investigation such events were found to be associated with the non-luminous structures within or adjacent to auroral bands, referred to as black aurora. They are furthermore found in regions of decreased ionospheric conductivity and magnetic field-aligned downward currents, and are necessary to close the system of adjacent upward and downward currents. The intense electric fields found in the present study are consistent with this theory. The higher occurence rate and intensity of the events at the higher altitudes suggest that a potential drop parallel to the magnetic field is might drive the downward current.

Chapter 1

Physical Background

1.1 Intro

The aurora is a visual phenomenon which can be seen most frequently in two regions encircling the magnetic poles of the Earth. However there is much more to the aurora than the eye can detect, and there are complicated processes that lay behind the sometimes very spectacular auroral formations. To understand what causes this phenomenon let us take a look at the physical situation around the Earth.

Some ingredients that are important for the creating of the aurora are the Earth's atmosphere, the Earth's magnetic field, the solar wind and the solar UV radiation. We also need some plasma physics to get the grip of things.

1.2 What is a Plasma?

A plasma is a gas or a fluid containing free charges such that the charged particles show some collective behaviour due to the electromagnetic forces caused by the presence of the charges. An individual charged particle must be influenced by the field from many other neighbouring charges. Phrased differently, the number of charges within a sphere of radius λ_D, the so called Debye length defined below, must be high. An electrolyte or a handful of electrons and ions thrown out into empty space are not examples of plasmas.

If a positive test charge is placed in an ionized gas, surrounding positive charges are repelled from, and negative charges are attracted towards the test charge as they move by. This results in a polarisation field that opposes the field of the test charge and effectively screens out the field from the test charge at a distance of one Debye length from the charge,

$$\lambda_D = \sqrt{\frac{\epsilon_0 k T_e}{e^2 n_e}} \tag{1.1}$$

where ϵ_0 is the dielectricity constant, k is Boltzmann's constant, T_e is the electron temperature, e is the charge of an electron and n_e is the electron or plasma density.

A plasma must have on the average essentially equal amounts of positive and negative charge, making the plasma quasineutral (diversions from exact neutrality correspond to electrostatic wave modes and boundary effects). Otherwise the electrostatic forces would be to strong to keep the plasma held together. The Debye length is also a measure of the largest distance over which quasineutrality can be appreciably violated.

Most plasmas in space have a very high electrical conductivity, and are very tenuous. The number density n is about 5 cm^{-3} in the solar wind and 50–100 cm^{-3} in the magnetosphere. The effect of direct collisions between particles can often be ignored compared to the effects of electromagnetic and other forces. Such plasmas are called collisionless. In the solar wind the mean free path between collisions is the same as the distance between the Sun and the Earth, 1 AU. In the ionosphere, on the contrary, the particle density is much higher, and the conductivity is finite and different in different directions relative to the magnetic field. More about the solar wind, the magnetosphere and the ionosphere later.

A charged particle moving in a homogeneous magnetic field describes a circular gyrating motion perpendicular to the direction of the magnetic field, and a constant motion along the field if there are no other forces involved. A quantity that remains a constant of the motion, when the magnetic field is changed arbitrarily slow is called an adiabatic invariant. One such quantity is

$$\mu = \frac{mv_\perp^2}{2B} = \frac{W_\perp}{B} \tag{1.2}$$

where $v_\perp$ is the component of the particle's velocity perpendicular to the magnetic field and $W_\perp$ is the part of the kinetic energy contributed by $v_\perp$. For a particle that moves along the field into a region where the magnitude of the field is higher, the velocity component perpendicular to the field must increase at the cost of the parallel motion, to keep μ a constant. If the field continues to increase the particle will finally reach a point where the velocity parallel to the field is zero, and all its kinetic energy is contained in the gyrating motion. The particle then cannot reach any further into the stronger field, but will turn back and gain more parallel velocity as the field strength decreases. This is called magnetic mirroring and the turning point is called the mirroring point. Particles can be trapped between two mirrors in a magnetic bottle, see Figure 1.1. The dipole field of the Earth provides a natural magnetic bottle. Particles with high parallel velocity compared to the perpendicular component will reach further into the stronger field before they are mirrored. If there is a maximum of the field strength, particles that reach beyond that point will not be mirrored back and are said to be lost. The angle α between the direction of the magnetic field and the particle's velocity is called the pitch angle, i.e. small pitch angle

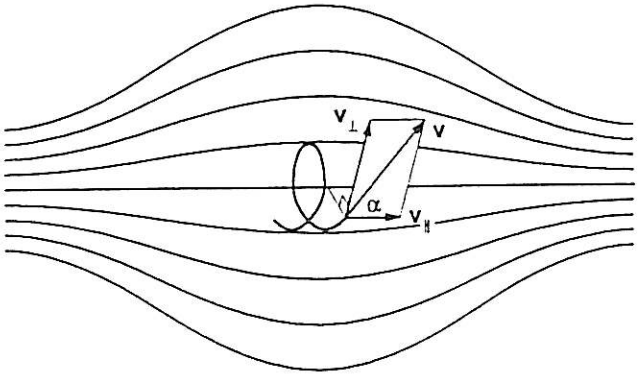

Figure 1.1: Particle movement in a magnetic mirror field

means nearly parallel motion. Particles with pitch angles small enough not to be mirrored back are said to be in the loss cone.

1.3 The Space Environment

1.3.1 The Geomagnetic Field

Not all planets have an intrinsic magnetic field, like the Earth has. The geomagnetic field is mainly caused by convective motion of the core. Within some Earth radii (R_E), the field is approximately a dipole field, but the magnetic field configuration is dramatically changed by the solar wind and the interplanetary magnetic field (IMF) that the solar wind carries with it. The strength of the geomagnetic field is 62 μT at the poles and 31 μT at the magnetic equator. The magnetic poles do not coincide with the geographical poles, and the best fitted centered dipole approximation places the magnetic north pole at 78.3° N, 291.0° E.

This difference between the magnetic dipole axis and the rotational axis makes the ordinary geographic coordinates inconvenient to use when the interest is focused on the magnetic field. The geomagnetic coordinate system is a spherical polar coordinate system fixed to, i.e. corotating with, the Earth, but with the polar axis along the approximated dipole axis. When studying phenomena that involves propagation along magnetic field lines, e.g. in auroral physics, the corrected geomagnetic coordinates suites better. These coordinates are a transformation of the geomagnetic coordinates using a higher order approximation of the geomagnetic field that better resembles the actual field. When the transformation is made, the actual field is represented as a simple dipole field

in the new corrected coordinates, making calculations a lot simpler.

The intrinsic geomagnetic field is not static but involves complex fluctuations, on long term and short term, large scale and small scale, due to the influence on the field from the Sun. At times when the fluctuations are large, it is said that the geomagnetic activity is high. Low geomagnetic activity is sometimes referred to as quiet geomagnetic conditions. One often used measure of geomagnetic activity is the so called K_p index. For each 3-hour interval the variations in the magnetic field is measured at several stations around the world. Measurements from twelve of those stations at geomagnetic latitudes between 48° and 63° is averaged, when first account is taken for the daily and seasonal variations, as well as the location of the stations making their measurements comparable. The result is the K_p index ranging from 0 to 9 in steps of a third of an integer: 0, 0+, 1-, 1 ,1+, ..., 8+, 9-, 9. High K_p means high activity.

1.3.2 The Solar Wind

The outer layer of the Sun, or the Sun's atmosphere, called the corona, is unlike the Earth's atmosphere continuously expanding outwards from the Sun. The corona is not itself luminuous, but it can be seen during a total solar eclipse, as it is lit up by the Sun's photosphere below it. Though the temperature of the photosphere is only about 6000 degrees Kelvin, the temperature at the base of the corona is very high, up to 10^6 K. Because of the high temperature the tenuous corona is totally ionized and consists mostly of electrons and protons plus alpha particles (Helium nuclei) that contribute about 16–20% of the mass of the corona. As the corona expands, the outflowing plasma becomes a supersonic solar wind, with velocities of 300–900 km/s. The speed of sound in the corona is only about 35 km/s.

According to the so called frozen-in-field concept, a moving plasma with high conductivity, σ, and the magnetic field lines within it move together. Two volume elements of the plasma that lie on the same field line will remain on that same field line as long as the conditions for frozen-in-fields hold. Expressed differently, the flux through a contour that moves with the plasma will remain constant. The condition is that the so called magnetic Reynolds number is high.

$$R_m = \mu_0 \sigma l_c v_c \gg 1 \tag{1.3}$$

where l_c and v_c are a characteristic length and velocity of the plasma. One assumption made in deriving the magnetic Reynolds number is that the time derivative of the electric field is small. The motion of the plasma and the magnetic field is governed by the relative strength of particle and magnetic energy. The Sun's magnetic field follows the flow of the more energetic solar wind. The flow is radially outwards from the Sun, but the rotating Sun as well as the solar wind drags the magnetic field with it, creating a spiral pattern of the field.

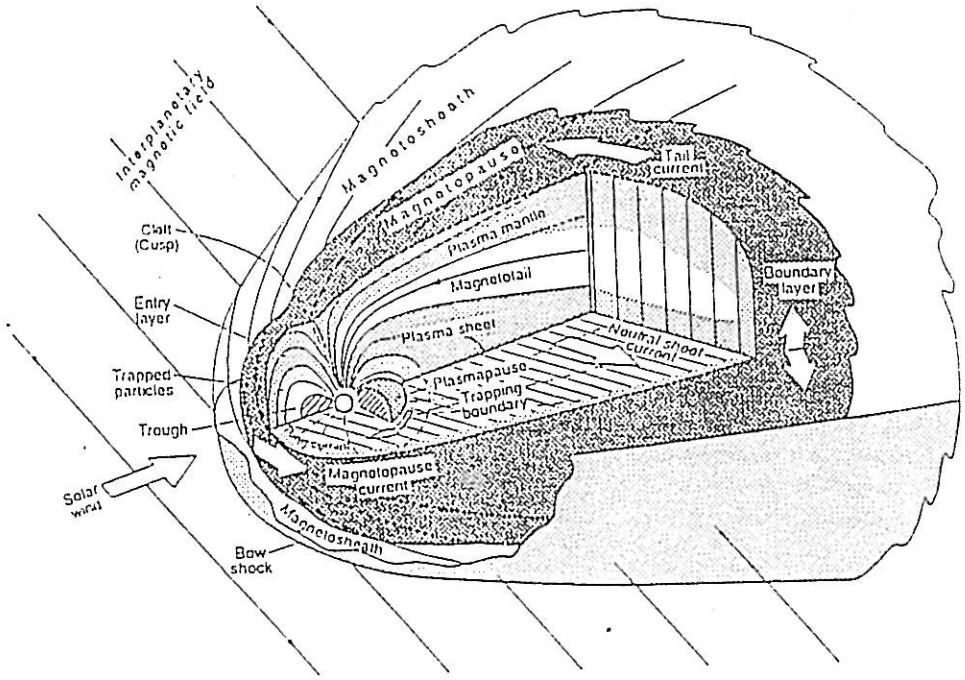

Figure 1.2: The Magnetosphere

This is the general structure of the solar wind and the IMF, but there are large variations in the solar wind temperature, density and speed, and in the magnetic field, due to sunspots, solar flares and events in the interior of the Sun.

1.3.3 The Magnetosphere

The region in which the magnetic field of the Earth dominates over the IMF is called the magnetosphere. Its boundary is a current layer called the magnetopause, and in the direction to the Sun it is found at a distance of typically 10 R_E. On the nightside the magnetosphere is stretched out hundreds of R_E in the magnetotail. The plasma in the magnetosphere comes originally from the solar wind and from the ionosphere. Figure 1.2 shows a schematic overview of the magnetosphere.

The Earth with its magnetic field acts as an obstacle to the supersonic solar wind flow, and a shock front, called the bow shock is created at about 14 R_E in the Sun direction. Unlike the shock wave from a supersonic airplane, the

bow shock is collisionless. Between the bow shock and the magnetopause is a region with subsonic plasma flow called the magnetosheath. In the region closest to the Earth the particle density is higher than in the further parts of the magnetosphere. This region is therefore called the plasmasphere, and it is contained within closed magnetic field lines emanating from low to medium high geomagnetic latitudes. Its outer boundary is called the plasmapause. During geomagnetic active conditions the boundary is quite sharp and during quiet conditions it is more diffuse. The so called Van Allen belts or radiation belts contain highly energetic particles that are trapped in the dipole field by magnetic mirroring. Due to their different masses the protons and electrons get trapped at different distances. In the inner belt at about 1.5 R_E protons with energies above 30 MeV are trapped. The outer belt at 3–4 R_E contains electrons above 1.5 MeV and reaches higher latitudes than the inner Van Allen belt. The origin of the trapped protons are neutrons that are thrown out from the ionosphere by cosmic radiation and decay into a proton, an electron and a neutrino. Trapped particles of lower energies exist almost everywhere in the magnetosphere apart from the most distant regions. Trapped particles are lost by collisions with ionospheric particles if their mirroring points are at low enough altitudes.

1.3.4 The Ionosphere

Below the plasmasphere with no distinct boundary is the ionosphere. It is the (partly) ionized continuation of the atmosphere, and stretches down to 60–70 km altitude. The ionization is mainly caused by short wave radiation from the Sun — UV and soft X-ray. Particle radiation is responsible for a lesser part of the total amount of ionization, but in the auroral zones it is the dominant cause of ionization. The lowest part of the ionosphere is mainly ionized by high energetic cosmic radiation. The electron density has its maximum at about 250 km altitude. At higher altitudes there are fewer particles to ionize, and at lower altitudes less of the solar UV radiation is left unabsorbed, making the degree of ionization lower.

The current sheet in the magnetopause does not completetely separate the IMF and the geomagnetic fields from each other. About 10% of the IMF penetrates into the magnetosphere. The interplanetary electric field is directed perpendicular to the magnetic field and to the direction of the solar wind flow. In the case of a southward IMF the coupling between fields looks schematically like in Figure 1.3. Field lines that emanates from the surface of the Earth and reenters on the opposite hemisphere are called closed field lines. Field lines which appear to have one end on the polar cap region and reach out beyond the magnetopause are called open. They do actually close somewhere far from the Earth, but for all practical purposes they can be regarded as open. The conductivity along geomagnetic field lines is mostly very high, which makes them approximately equipotential lines. Therefore the interplanetary electric field maps along open field lines to the polar caps. This approximation does

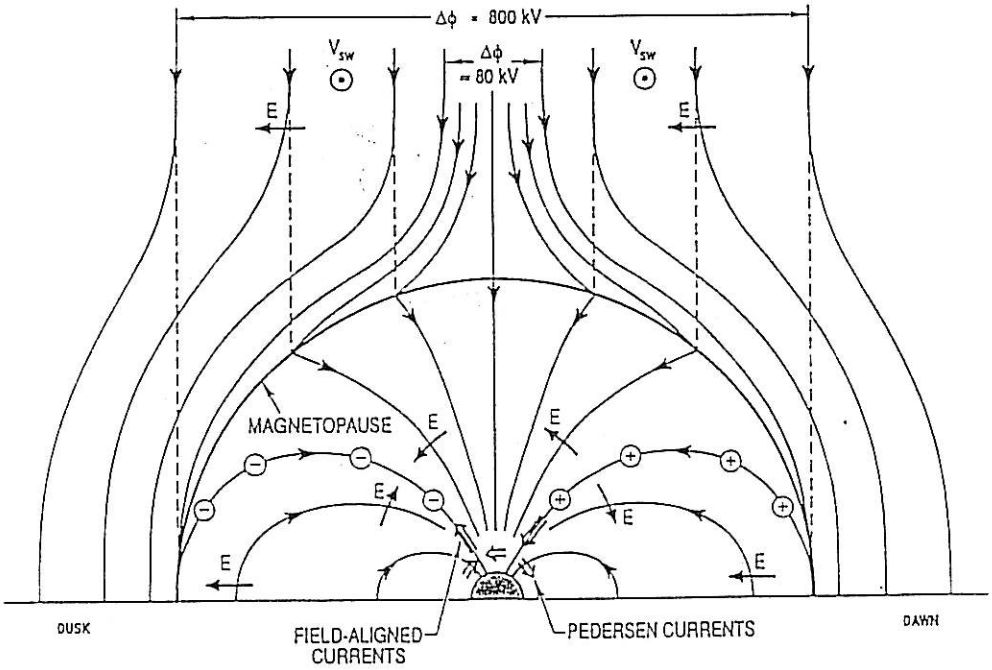

Figure 1.3: Illustration of how the IMF couples to the magnetosphere, showing magnetic field lines emanating from the dawn-dusk meridian projected onto the dawn-dusk meridian plane. Solid lines show the field under the assumption that 10% of the IMF penetrates the magnetopause. Dashed lines show the field as if the entire IMF would penetrate the magnetopause. Also shown is the charges and electric field along the boundary between open and closed field lines. Currents are marked by open arrows. The picture is taken from [Lyons, 1992]

not always hold, and the existence of field-aligned (i.e. parallel to the magnetic field) electric fields are essential for the creation of the aurora.

1.4 The Aurora

What we see as the aurora is the emission of visible light from ionospheric atoms and molecules that are excited by precipitating energetic magnetospheric particles, mostly electrons but also protons. The light is emitted at heights between 100 and 200 km. Auroral emissions most frequently occur between 65 and 75 degrees geomagnetic latitude. Those regions, one around each magnetic pole, called the auroral zones are where aurora statistically is most observed. The actual extension of the aurora at a specific time is also a region encircling the pole, but tilted towards the nightside of the Earth. This so called auroral oval varies in size and location with the geomagnetic activity. At times with higher K_p the oval is stretched out to lower latitudes. During low activity the oval will shrink, but it will always remain an oval. Sometimes a band of auroral luminuosity also stretches across the polar region from the nightside of the oval to the dayside. This structure is called a transpolar arc.

The colour of the aurora depends on the spectral lines and bands of the excited atoms and molecules. Mostly the dominant spectral line is 5577 Å from oxygen atoms, making the aurora greenish yellow. Emissions in the red part of the spectrum are also common. If the light is too faint, the human eye cannot detect any colours, and the aurora will appear as white to an observer.

The aurora can appear in many different forms, and at different altitudes. The higher the energy of the precipitating electrons, the deeper they can penetrate into the ionosphere/atmosphere. Electrons entering the ionosphere from different regions of the magnetosphere can reach quite different energies, see Figure 1.4. Another distinction is made between structured and diffuse aurora. The structured or discrete aurora is when the light emissions is formated in those varying shapes and colours that we mostly think of as the aurora. The diffuse or continuous aurora is less spectacular and appears in east-west aligned bands or arcs of quite uniform luminuosity. Next to, or inbetween two adjacent arcs are often found regions with almost no emission, referred to as black aurora. Despite its more modest appearance, the diffuse aurora contributes most of the energy input to the ionosphere in the 1–10 keV region. The diffuse aurora can result from both electrons and protons, whereas the discrete aurora results from electrons alone.

The aurora can also be classified through the pattern of the electric field across an auroral arc, e.g. by how the electric field strength is correlated or anticorrelated to the particle precipitation. Marklund, [1984], presents an auroral arc classification scheme, where the division is not only based on the morphology of the electric field pattern, but includes the physical mechanisms involved. The different classes are grouped into two main categories, after how current conti-

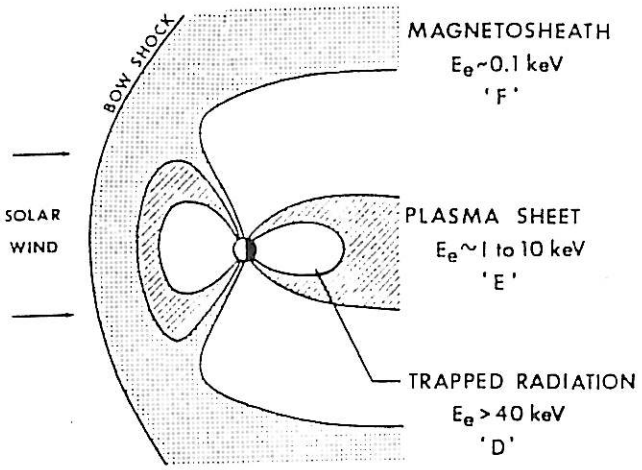

Figure 1.4: Noon-midnight cross section of the magnetosphere showing schematically the principal source regions for electrons of different energies. Together with the electron energy, the ionospheric region in which the particles produce maximum ionization is given. These regions are labelled D, E and F, where D is the lowest part of the ionosphere, and F the highest. The Illustration comes from [Whalen, 1985]

nuity is maintained across the arc, by polarization electric fields or by Birkeland currents, which is the same as field-aligned currents (FAC).

The precipitating electrons that causes the aurora enters the ionosphere essentially along the field lines of the Earth's magnetic field. However, thermal electrons do not provide enough energy to produce the aurora, and low-energetic electrons will be reflected by the magnetic mirroring force before they can penetrate deep enough into the ionosphere. Therefore there must be some acceleration process(es), in which the electrons gain velocity in the direction of the magnetic field. Parallel acceleration will increase both the energy of the eletrons and the number of electrons within the loss cone. This may be done if there is a potential difference which the electrons can pass on their way down, i.e. they are accelerated by field-aligned electric fields. How these electric fields are maintained is not a fully solved question, but the potential curves are suggested to be U-shaped, a few kilometers wide, located above the auroral arcs. Recent satellite observations give further clues to this question, see section 2.2

Chapter 2

Previous Results

2.1 Before Freja

Strong electric fields have been found in the auroral oval at higher altitudes by earlier satellite missions. Bennet *et al.* [1983], report on measurements made by the S3-3 polar-orbiting satellite at altitudes ranging from 240 up to 8000 km. The electrostatic shocks, as they called strong field events with $E > 90$ mV/m, occurred in connection to the auroral oval, with the most equatorward shocks occuring when the K_p value was high. This is in accordance with how the extension of the auroral oval varies with magnetic activity.

Most of the events occurred above 4000 km, and events at altitudes below 4000 km occurred more frequently during winter than summer. In winter the ionosphere is less exposed to ionizing solar radiation, which was thought to be the reason of the observed difference between the seasons. High values of K_p also increased the probability of finding strong fields at lower altitudes, which was explained by field-aligned currents increasing with K_p.

The occurrence of shocks were found to be correlated to the occurrence of upward flowing ion beams and ion conics, i.e. they were correlated to parallel potential drops. The most energetic ion beams were those who were most associated with strong electric field events, indicating a treshold potential drop for the formation of electrostatic shocks.

The two satellites DE 1 and DE 2 measured the electric field simultaneously at different altitudes. Weimer *et al.* [1985] compares data from the DE satellites at times when there were approximately on the same magnetic field line with DE 1 mostly above 4500 km altitude and DE 2 below 900 km. The measured electric fields were mapped to a common altitude to make the comparison possible. Fourier transform made it possible to distinguish between field structures of different length scales. It was found that the large scale fields were the same at both altitudes whereas the fields associated with small scale structures —

less than 150 km — were greater in magnitude at the higher altitude. These small scale structures appeared in connection to the aurora and the difference in magnitude was interpreted as the existence of a field-aligned potential drop. This difference was also found to be correlated to large flux of electrons down the field lines and high ionosperic conductivity. Outside the auroral zone the mapped electric fields from DE 1 and DE 2 were nearly identical.

DE 1 covered altitudes from 1.1 R_E to 4.6 R_E, and a study was made of the electric field data, both of strong field events and of the average field, [Weimer and Gurnett, 1993], showing an altitude dependence of the mapped electric fields that confirmed the existence of parallell potential drops at auroral latitudes. Most of the fields stronger than 100 mV/m were found above 2500 km up to 10000 km and tended to have a convergent structure. The largest field that was found was 844 mV/m (unmapped value) at 1.45 R_E and had a divergent structure. The space scale was smaller than for the general event and the field was embedded within the field-aligned upward current sheet that was associated with it. The converging fields appeared at higher altitudes and were spatially larger, with the upward current sheets inside the field structure. Weimer and Gurnett suggested that the strong diverging field was caused by a low frequency wave.

The first Swedish satellite Viking also found strong converging electric fields, associated with parallel potential drops. Viking was operating in a nearly polar orbit between 800 and 13500 km altitude.

2.2 Freja Observations at Higher Altitudes

With the launch of the Freja satellite new advantages in measuring the electric field at low altitudes were given. The orbit was such — 63 degrees inclination — that the satellite spent more time in the auroral oval at each crossing than for a polar orbit. The high sampling rate and telemetry rate and the possibility to store data, enabled the collection of high resolution data from both hemispheres. In normal mode the temporal resolution was 1.3 ms. Apogee was at 1760 km and the parallel potential drop mostly does not reach down to these altitudes, and thus strong converging fields were not expected to be found to any great extent. What instead was found were strong electric fields with a divergent structure. Marklund *et al.* [1994] and Marklund *et al.* [1995a,b] report on strong field events in the northen hemisphere auroral zone. They conclude that they are associated with black aurora between or adjacent to auroral bands. The properties of black aurora coincide with what is found in association to the strong diverging fields. The strong fields appear in regions of decreased conductivity and very low electron precipitation next to regions of high electron precipitation. Also found are perpendicular ion fluxes, and downward field-aligned currents.

The Freja observations of strong diverging fields, together with earlier observations, suggest that the system of electric fields and currents above the aurora

can look like in Figure 2.1 in the case of two auroral arcs with a black aurora inbetween. In the black auroral region the plasma density is low leading to a low conductivity as well. Between the upward field-aligned currents — due to downward accelerated electrons — there is a downward FAC to assure current continuity. To close the system there are perpendicular currents between the arcs, i.e. within the black aurora. Because of the low conductivity in that region strong fields are needed to drive the perpendicular currents there.

Black auroral bands can develop vortex street structures of black auroral curls and one example is given by Marklund *et al.* [1994] of an event that could be assosiated with such black auroral curls. It is also suggested that the event explained by Weimer and Gurnett by low frequency waves, might be explained by curls of black aurora.

While Marklund *et al.* argued that auroral bands and black auroral bands next to each other result in the current system in Figure 2.1, Doe *et al.* [1995] approached the situation the other way around. They used an ionospheric model with two oppositely directed field aligned currents, and their result was that such a current system could create density depletion cavities.

Johnson and Chang [1995], used a model of a black auroral curl as a drifting two-dimensional vortex like electric field structure within an elongated density depletion. When using parameters characteristic of the auroral region at 1700 km altitude, the result of their calculations was electric fields of the order of 1 V/m and the spatial scale of the structures was of the order of 1 km. Electric fields of that strength and size was found by Freja at the same altitude.

One case of black auroral dark filaments was studied by Schoute-Vanneck et al. [1990], using high resolution TV-cameras. The width of both auroral bands and dark regions where typically 1 km. The east-west dimensions of the dark bands were 5 to 20 km. The dark filaments were drifting eastwards with an average velocity of 2.3 km/s, while the $E \times B$-drift at the time was $\leq$ 0.3 km/s. The luminuosity of the dark bands was close to that of a clear night sky.

A study of 7–8 months Freja data was made to investigate the occurance and characteristics of the strong field events. The data used were from the northern hemisphere, i.e. altitudes near apogee at the auroral crossings. Field strengths of 200 mV/m and more were considered as events. As expected the geographical distribution was concentrated to the auroral region, with events at lower latitudes occurring at times with higher K_p. The strong fields were shown to be associated with low ionospheric conductivity, since the majority of the events as well as the strongest fields were found near midnight and in the early morning sector. The strongest fields were also found near winter solstice. The events were found to be correlated with perpendicular ion heating and anticorrelated with field aligned electron precipitation. A connection was observed between amplitude and scale size of the events; the strongest fields had the smallest extension — a few km — whereas the spatially largest strong fields were typically less than 500 mV/m. Due to this it was suggested that there might be a treshold for the potential difference across the diverging field

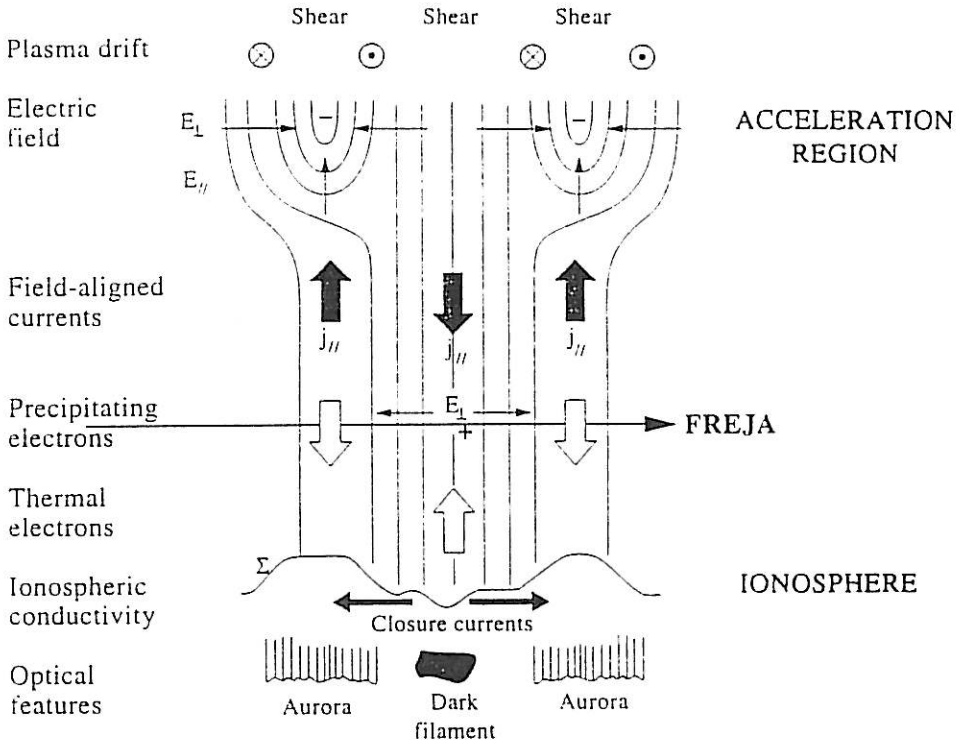

Figure 2.1: Possible configuration of equipotential lines, electric field, currents, electron motion and conductivity in connection to a double arc system with an interjacent dark auroral band. Note the converging electric fields in the acceleration region and the diverging field at Freja altitude.

structure, determined by the potentials of neighbouring auroral arcs. All these observations support the idea that the strong diverging fields are associated with black auroral bands and the vortex streets of black auroral curls that can arise when black bands go unstable. It was suggested that such diverging fields should exist also at other altitudes, and one example was given of an event measured by Freja at 840 km altitude. Strong diverging fields might also be found at higher altitudes if e.g. Viking data were examined more thoroughly. The work presented here is the continuation of the Freja investigation at lower altitudes.

Chapter 3

Electric Field Data Analysis

3.1 Instrumentation

The Freja scientific satellite was launched on October 6, 1992. It was put into an orbit with 63 degrees inclination and an altitude range between about 600–1750 km. The instruments onboard provide measurements of the electric and magnetic fields, the plasma density, particle fluxes etc. The telemetry rate is normally about 260 kbits/s and is sometimes doubled to 520 kbits/s, and data can be recieved at two ground stations: at Esrange, Sweden and Prince Albert, Canada. Freja can also store data on board, making it possible to get data also at times when neither of the two ground stations can be reached directly, e.g. at southern hemisphere auroral crossings.

The on board memory can also be used to collect data at a higher rate than the telemetry rate. In burst mode the sampling rate can be 2 Mbits/s during one minute. The are four different modes for data taking corresponding to different sampling rates. The burst mode with a sampling rate of 6144 s^{-1} can be used to get high-resolution data of discrete auroral arcs. In normal mode data can be collected for 9 minutes before the memory is full. For the electric field experiment this means a sampling rate of 768 s^{-1}, corresponding to a time resolution of 1.3 ms. This mode is suitable for collecting data from one auroral oval crossing, see Figure 3.1. In the normal mode the sampling rate and telemetry rate are equal. To obtain data from entire orbits the compressed and overview modes are used.

Freja is equipped with six spherical probes mounted at the tip of wire booms in the spin plane of the satellite as shown in Figure 3.2. Two, four or sometimes all of the probes are used to measure the electric field. For the data studied here probes 1 to 4 have normally been used. The quantity that Freja records in the

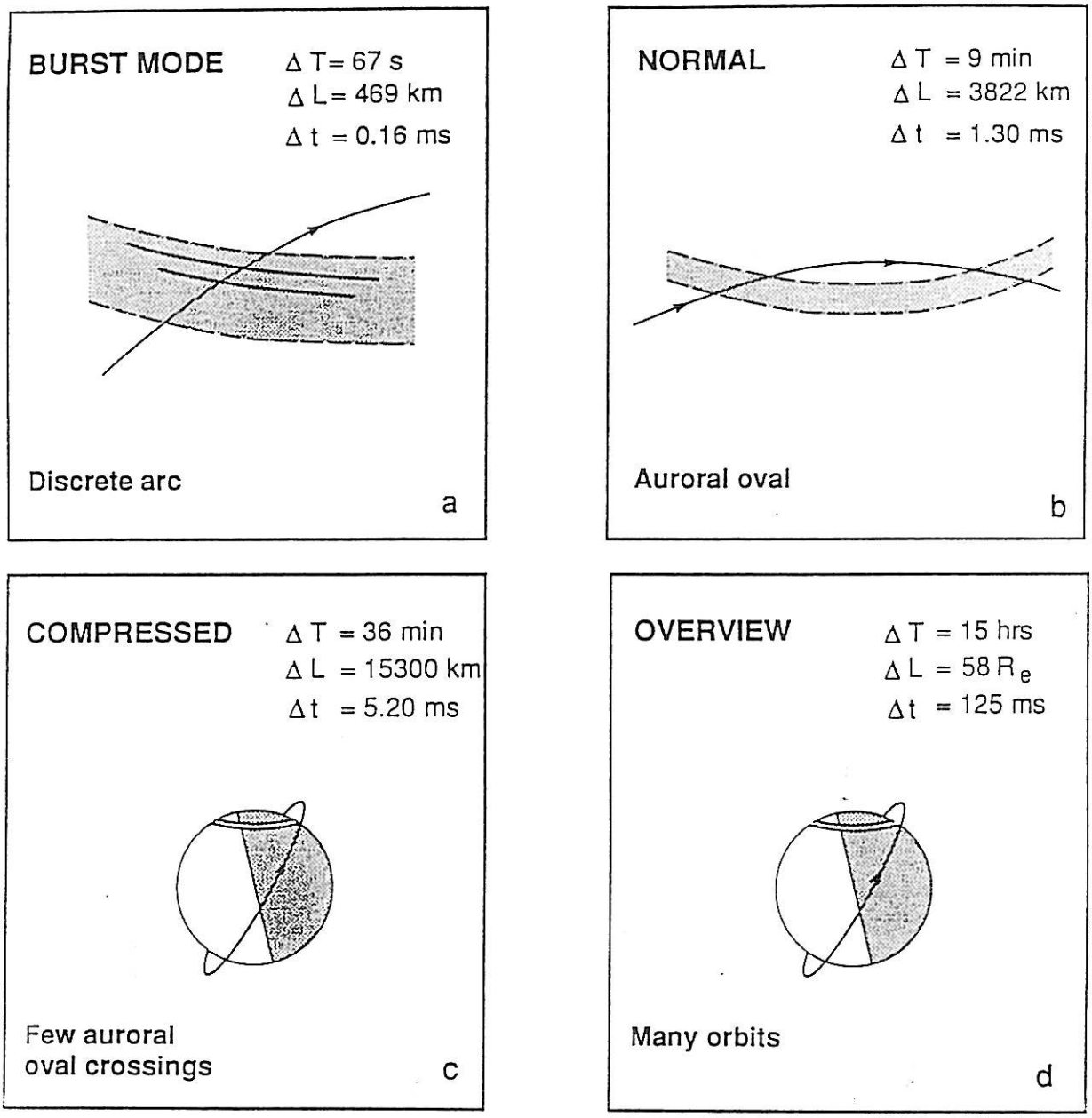

Figure 3.1: Electric field experiment modes of operation

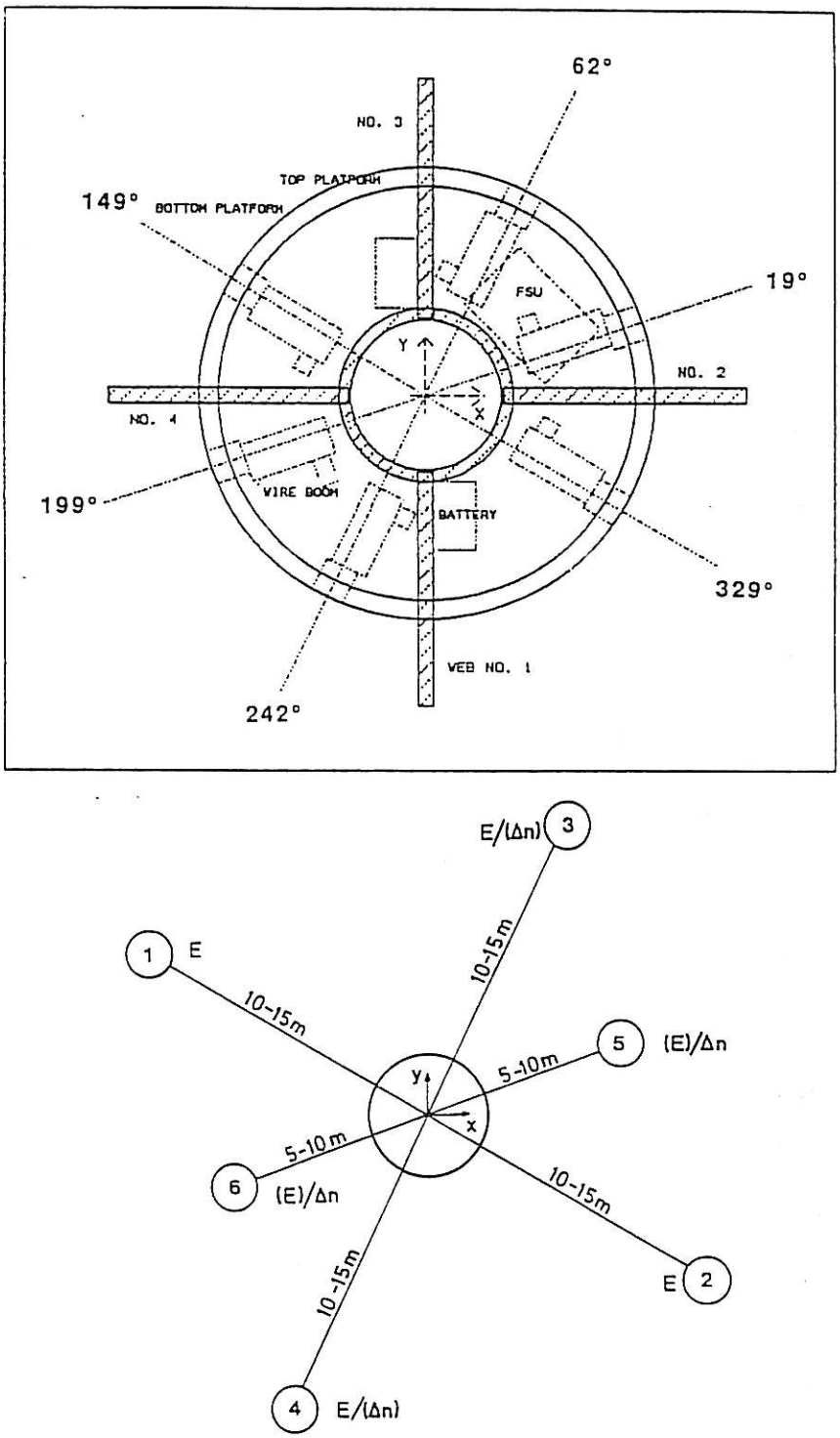

Figure 3.2: Wire boom and probe configuration

electric field experiment is the potential difference between the individual probes and the satellite body, as well as the potential difference between opposing probes. The average of the potential of selected probes — normally probes 1 and 2 — called the floating ground potential, V_{fg}, is calculated. To make the measurements as accurate as possible the probes are kept close to the potential of the ambient plasma by applying a bias current to the probes. This makes V_{fg} an approximation of the satellite potential, but with opposite sign. To decide the optimum bias current, current sweeps are made, where the bias current is swept from +950 nA to −534 nA in about 300 ms. The interval between the current sweeps is of the order 30 s. It was found that a small positive bias current held constant at 22 nA could serve well for most situations. The current-voltage characteristics of the sweeps can also be used to determine the plasma temperature and density, see [Lindqvist *et al.*, 1994].

3.2 Method

3.2.1 Collecting and Processing the Data

The area of interest in this study is where Freja has its perigee, which is over the southern hemisphere for the data studied here. Thus the orbits to look for were those containing data in stored normal mode. In 1993 such data were produced only during six orbits, none of which contained strong electric fields. In the 1994 data set more than 300 orbits contained the appropriate data type, and that would be enough for a statistical study, provided sufficiently many of them contained strong fields. For this to be the case the treshold for labeling a peak in the electric field as a strong field, had to be lowered from 200 mV — as in [Karlsson and Marklund, 1996] — to 100 mV/m. With this limit 69 events of intense electric fields were found in the 1994 data.

For each orbit a plot of the E-field was produced. The raw data from the electric field experiment is the voltage between the satellite probe pairs. To estimate the actual electric field from that, first the current sweeps are detected and subtracted. The next thing, which is of more physical importance, is that one has to subtract the $\vec{v} \times \vec{B}$-contribution to the field arising from the satellite motion — rotation and translation.

Together with the E-field, plots where also given showing the potential (as calculated from the measured E-field), the angle between the spin-axis and the magnetic field line, and whether the Sun was in eclipse or not. Additional information given on the x-axis was time (UT), altitude, Corrected Geomagnetic Latitude (CGLat), Magnetic Local Time (MLT) and geographic latitude and longitude. For those orbits where the absolute value of the E-field appeared to be near (with good margin) or above 200 mV/m, plots of the raw data — V_{12}, V_1, V_2, V_{34}, V_3 and V_4 — were also produced, unless it was obvious that the high value of the field was due to erroneous data. Raw data plots were also

made in doubtful cases, e.g. when an erroneous peak in the field was so high that it was impossible to see if there were any strong fields in the rest of that orbit. Some of the plots are presented in section 3.3.1.

The scale size of an intense electric field structure was obtained in the same way as for the northern hemisphere investigation at higher altitudes. The half-width of the largest spike was measured and multiplied by 4, since it was found in the northern hemispere data that the spikes often appeared in pairs, oppositely directed. The scale size was then scaled to a common height of 100 km. This is done since the electric field structures can be mapped to ionospheric heights following the magnetic field lines assuming $E_{\parallel} = 0$, and the dipole structure of the magnetic field makes it necessary to rescale the scale size. The mapping to a common height makes it possible to compare measurements at different altitudes. Of special interest is to compare the results from this investigation of Freja data to that performed earlier by Karlsson and Marklund [1996].

In many orbits the measured E-field values were not centered around zero, and thus the offset had to be subtracted to get the correct absolute value. This happened most often during eclipse. Freja uses the direction to the Sun to keep track of in which phase of the rotation the satellite is. The phase is then used to make the $\vec{v} \times \vec{B}$-correction of the electric field.

The correction for the offset was done by calculating the average of the field data over evenly spaced intervals. In the middle of each interval, the offset was set to the averaged field strength in that interval. Between the midpoints of two adjacent intervals the offset was interpolated linearly. It was during this process that it turned out that a lot of the candidates for strong field events actually were lower than 200 mV/m but could still be considered strong since they exceeded 100 mV/m. To get more data to work with the latter value was henceforth taken as the treshold for strong fields. This leaves a possibility that some of the previously rejected data could contain strong fields, but that would not change the overall statistics.

The satellite probes only provide the field in the spin plane and therefore some assumption has to be made about the spin axis component of the field. In this case it is simply set to zero, to avoid making assumptions that might not be physically valid and to avoid overestimating the field. This of course means that we would fail to register large fields where the spin axis component is large but the spin plane component is less than 100 mV/m.

3.2.2 Selecting the Intense Fields

To make sure that high values in the output E-field data really represented strong fields, each suspected intense field event was checked against the raw data, both the potential difference between opposite probes and the potential for each individual probe. For this purpose new more close-up plots were made. Sources of erroneous field data were found to be gaps in the raw data, saturation of the probes and effects due to the current sweeps. Structures in the E-field

with periodicities equal to a quarter of, a half or a whole spin period were also considered as false data.

Given the electric field, the potential was calculated to determine wether the structure of the intense fields were divergent or convergent or neither. A local maximum in the potential implies a local excess of positive charge and a diverging electric field, the opposite situation for a local minimum. The plasma is of course assumed to be neutral averaged over a larger scale. Unfortunately, the software used did calculate the potential simultaneously with the electric field, i.e. before the field was corrected for the drifting offset. Thus for those events occurring in an orbit with a (large) non-zero offset, the result was a monotonically increasing or decreasing potential curve from which it was hard or impossible to detect any deviations due to diverging or converging electric fields.

As a further check the field and potential were also calculated according to the assumption that the component of the electric field parallel to the magnetic field was zero. Using this assumption did not change the occurrance of the strong fields — though often changing slightly the magnitudes and directions of the peaks — and did not change the major structure of the potential curves.

For the five strongest events the electric field data were transformed to a coordinate system with one axis along the magnetic field and the other two perpendicular to the B-field and directed towards magnetic east and equatorwards, respectively. Since we are mainly interested in structures perpendicular to the magnetic field, we can use the two latter components to detect divergence of the intense electric fields. For this special study of the most intense fields a higher resolution of the data was used, which was not necessary for the statistical survey.

3.3 Observations

In the 1994 southern hemisphere electric field data 69 events of electric fields with a magnitude of more than 100 mV/m were found at altitudes between 640 and 1026 km. The strongest field was 1827 mV/m. The five strongest electric field events are presented below. The distribution and some statistical properties of the collection of all 69 events are presented in summary plots following the lines of the higher altitude Freja investigation, presented by Marklund *et al.* [1995a].

3.3.1 The Strongest Fields

The five strongest events occurred between Aug 18 and Sep 13, i.e. during late winter in the southern hemisphere. They also occurred near magnetic midnight within the period 23.30 to 02.00 MLT.

In orbit 9008, Aug 18, 1994, Figure 3.3, a structure of large fluctuating fields

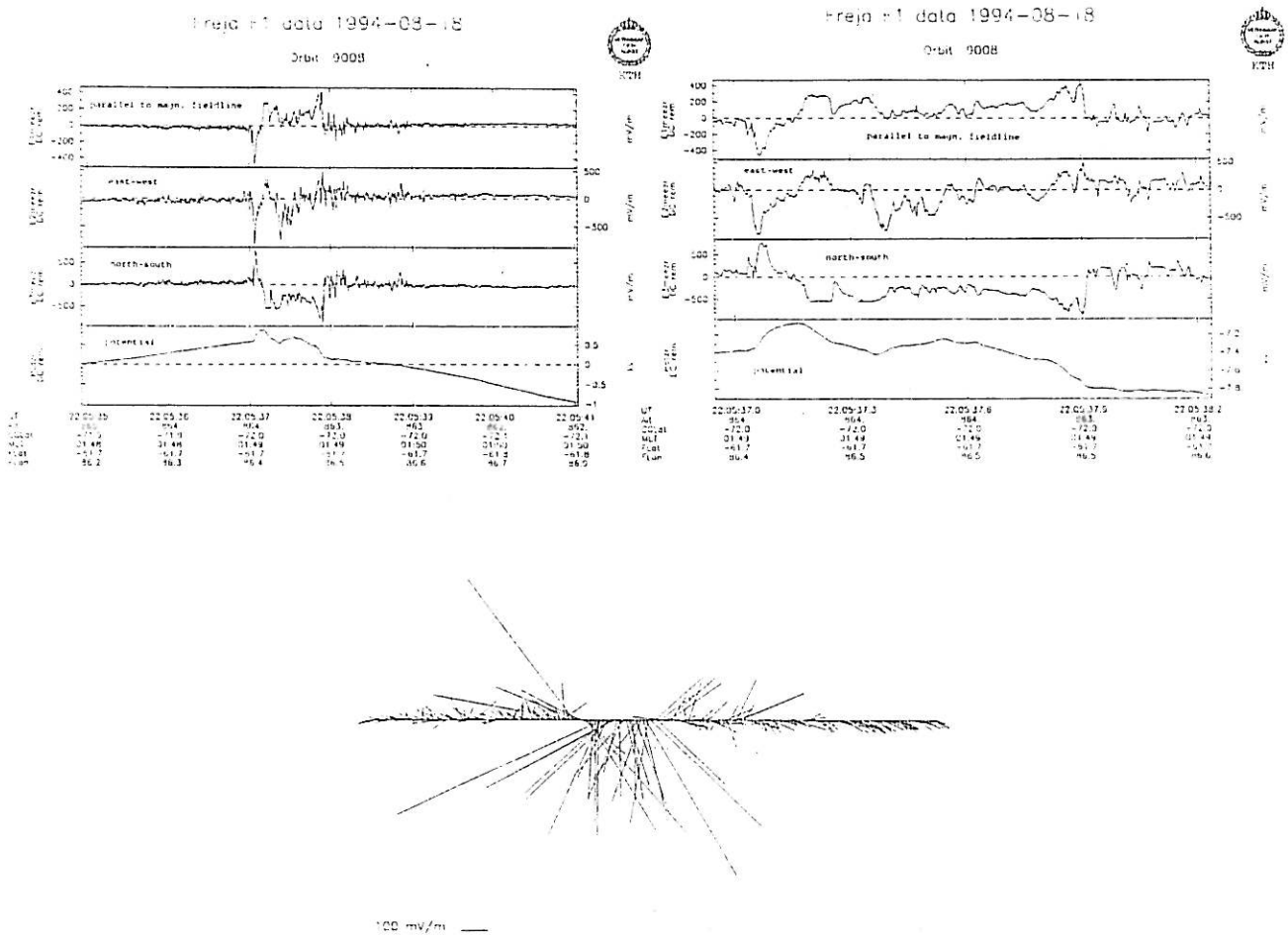

Figure 3.3: *Top left:* The electric field and potential from part of Freja orbit 9008. The components of the electric field are field-aligned, east-west and north-south. The potential is calculated from the electric field data. *Top right:* A more close-up view of the same event. *Bottom:* A plot of the electric field vectors projected on the plane perpendicular to the magnetic field. Same range as top left.

was observed. It extended for about 10 km of the orbit, and was surrounded by comparably weak fields. Large fluctuations are seen in the east-west direction. There is a large southward component over the whole structure except at the boundaries where the north-component is dominant. The strongest peak is 1135 mV/m, at 22:05:37.1 UT, right at the western edge of the structure. At the eastern end of the structure, at 22:05:37.9 UT, there is another strong peak reaching 1000 mV/m. The electric field data at this point could have been affected by a period of 0.3 s of probe saturation starting at 22:05:37.9 UT. Nothing was found to be wrong with the rest of the data. It can be seen from the potential curve and from the electric field vector plot, that the structure as a whole is divergent, likely to consist of two divergent structures next to each other. At 22:05:37.4 UT, close to the potential minimum between the two potential 'hills', the electric field has a large westward component.

In orbit 9139, Aug 28, 1994, Figure 3.4, there is a lot of distorted data, often due to probe saturation. Their repeated structure makes them easy to distinguish from the real strong fields shortly after 19.58 UT. There is a clear local potential maximum in the region of strong fields, with its maximum at 19:58:14.4 UT. The strongest peak that was measured when there was no doubt about the quality of the raw data was 1077 mV/m, and had a large east-component. It is located at 19:58:14.5 UT, where the potential curve has a negative slope.

In orbit 9175, Aug 31, 1994, Figure 3.5, the strongest field is 1082 mV/m, and the structure has a double peak, a few km wide, both peaks dominantly pointing north-west, with no large ambient fields. The larger of the two peaks is about three times stronger than the weaker. The electric field structure is very smooth, with no small scale fluctuations superimposed on the general structure. This event is the one found at the highest altitude, 1026 km. It is also one of the most equatorward events with CGLat $-66.2°$. There is a large step in the potential in connection to the electric field event, but an offset of about 200 mV/m makes it difficult to tell wether the field is diverging or not.

In orbit 9335, Sep 12, 1994, Figure 3.6, there are strong varying fields for about a minute — nearly 500 km — with the largest fields in the first part of this period. In the middle of the structure, the fluctuations are of smaller amplitude than at the edges. There is a large offset of about 400 mV/m making it hard to interpret the potential curve or the vector plot of the field. The largest peak is 427 mV/m and is of the order 10 km, stretching from 15:54:47.4 UT to about 15:54:48.4 UT where there is a short period of more high frequent variations. The field reaches its maximum at 15:54:48.2 UT. The East-component is dominant throughout this 10 km wide event. There is also a double peak structure in the north-south direction, but very little can be seen in the east-west component. This structure has about half the field strength of the larger event.

In orbit 9348, Sep 13, 1994, Figure 3.7 is found the by far largest field, 1827 mV/m, at 15:31:52.84 UT. There is actually a peak of more than 3000 mV/m

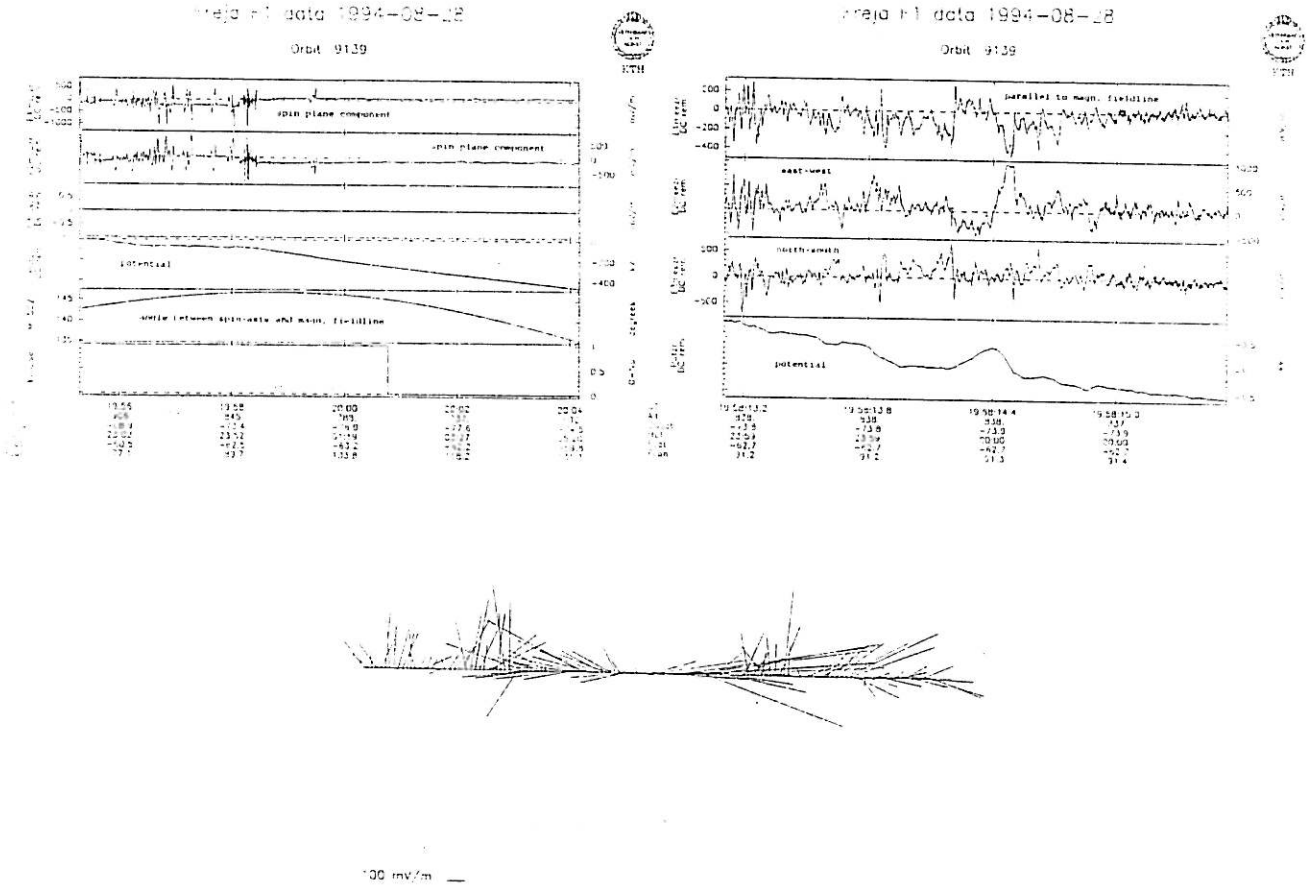

Figure 3.4: *Top left:* Orbit 9139. Panels showing spin plane components of the electric field, potential, angle between spin axis and magnetic field, and whether Freja was in eclipse or not. *Top right:* Part of region with strong fluctuating fields. Components are magnetic field-aligned, east-west and north-south. *Bottom:* vector plot over the electric field. Same range as top right.

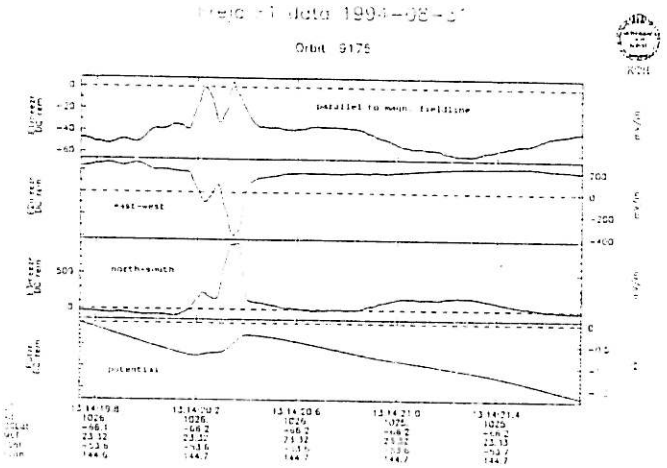

Figure 3.5: Strong field event in orbit 9175. Large offset in the data.

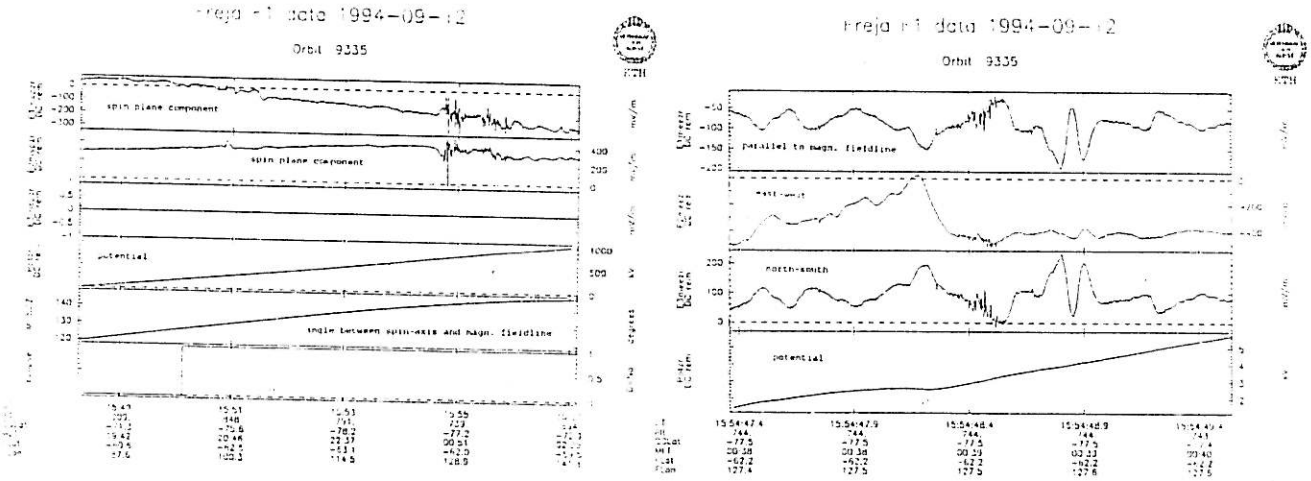

Figure 3.6: *Left:* All normal mode data from orbit 9335. *Right:* In this plot the electric field is not corrected for the large offset. The strongest peak is found at 15:54:48.2 UT.

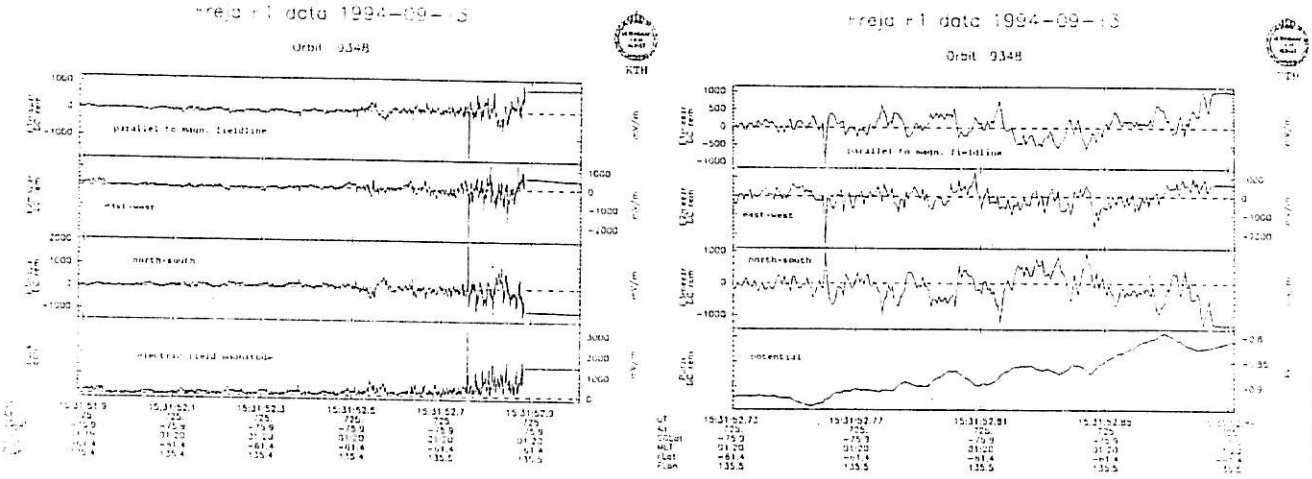

Figure 3.7: *Left:* Very large fluctuating electric fields in orbit 9348. Bottom panel shows the absolute value of the electric field. *Right:* A more close-up view of the strongest fields. *Note* that the spike reaching over 3000 mV/m is a false data point.

in the data but that peak is considered false[1]. The largest real peak is found in a region of very fluctuating and strong fields in all directions,on a short time scale. The largest fluctuations occur in a region of about 1 km, with ambient smaller amplitude fluctuations extending over 10 km. A large gap is seen in the data, shortly after the satellite had encountered the strongest fields. During the strong fields the potential has several maxima and minima.

3.3.2 Statistical Survey of Events

In the higher altitude investigation four plots were made, showing the geographical distribution of the events, and the relation between some of their properties. To compare the results of the present investigation with the previous by Karlsson and Marklund, the same kind of statistical survey plots where made. They will be presented together with the plots of the northern hemisphere data. For convenience the two sets of plots will be referred to as N-plots and S-plots respectively. Besides that the measurements are made at different altitudes, two other important differences in the indata should be noted. The number of events is smaller in the southern hemisphere data and the treshold used to define an event is 100 mV/m in this study, but 200 mV/m in the previous. In both cases the

[1] It suddenly appeared after a transformation of coordinates.

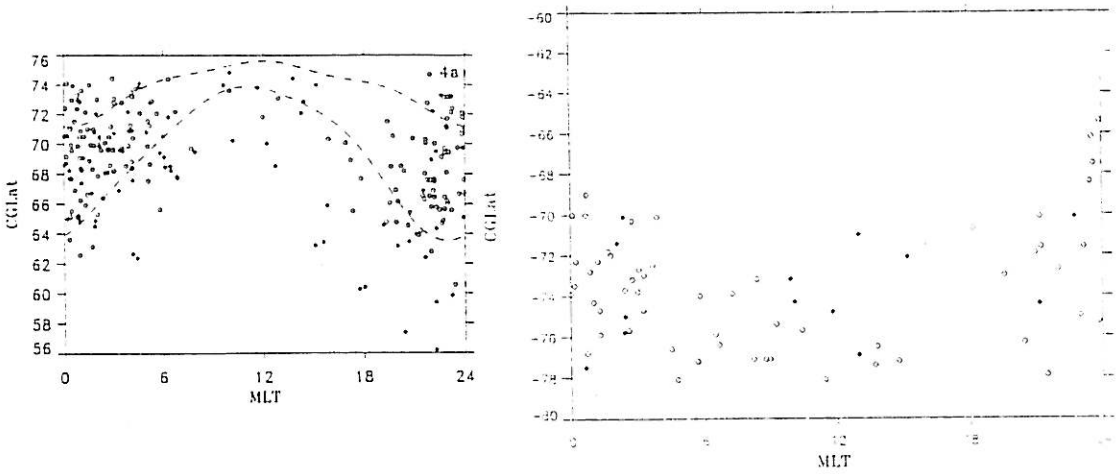

Figure 3.8: All events marked in a CGLat vs MLT diagram. Filled and open squares are events occuring during $K_p > 3$ and $K_p \leq 3$ respectively. *Left:* Northern hemisphere events from altitudes around 1700 km. *Right:* Southern hemisphere events from altitudes around 800 km.

events are represented by filled squares when the K_p value was greater than 3, and open squares for K_p below or equal to 3.

Figure 3.8 shows the occurence of the events in a CGLat versus MLT coordinate system. The average location of the auroral oval for moderate activity level is marked by dashed lines. In both plots the events are concentrated mainly to the auroral region. Events occurring during high K_p tend to be located more equatorward, which is consistent with the broadening of the auroral oval at active times.. This is most evident in the N-plot where it can be seen at all local times, but quite obvious also for the dayside sector in the S-plot.

Figure 3.9 shows the intensity of the electric field vs MLT. In both studies the strongest fields occur in the night and morning sector, but in a much more narrow local time sector in the southern hemisphere data. The larger spread in the N-plot may partly be a consequence of the larger number of events. In the S-plot the five strongest field events are found between 23.30 and 02.00 MLT. The more modest events occur for all local times in both cases. Furthermore, the most intense fields occurred during low activity at both altitudes.

Figure 3.10 shows the electric field intensity vs scale size. In the S-plot there are events with scale sizes up to 290 km, while no event in the N-plot exceeds 25 km, which is likely to be due to the different treshold values used. Almost all of the largest sized fields in the S-plot have a field strength less than 200 mV/m. To simplify comparison with the N-plot, a second S-plot is made excluding events with scale size larger than 25 km. Doing so the pattern of the

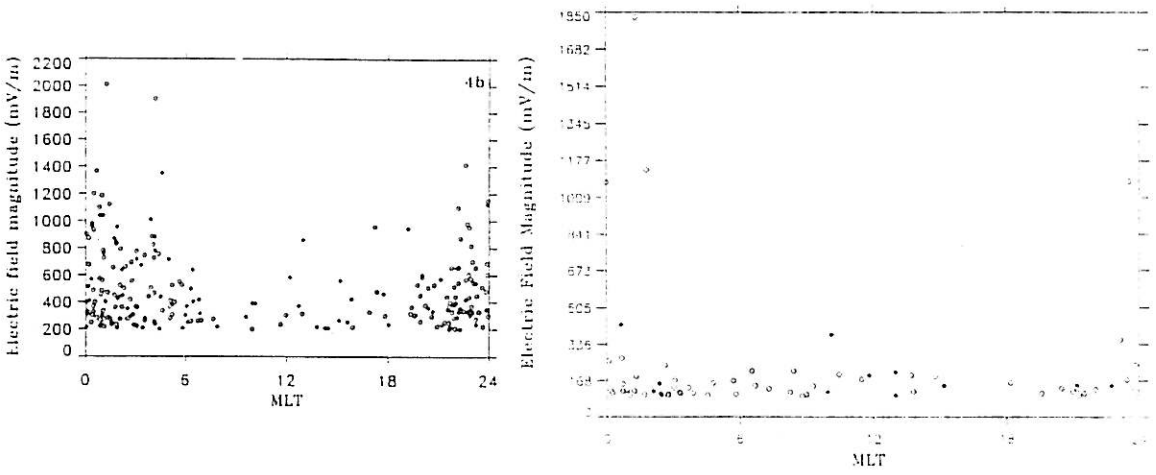

Figure 3.9: Electric field vs MLT. *Left:* Higher altitude data. *Right:* Lower altitude data.

S-plot resembles more that of the N-plot. The events with the strongest fields tend to have smaller scale size. The most intense event is seen to have a scale size of about 2.5 km. However, larger fields at even smaller scale sizes may exist since the appearent lower limit of about 2.5 km size is due to limited resolution.

In Figure 3.11 the scale size is plotted vs MLT. As above two S-plots were made with different range on the scale size axis. The fields with very large scale sizes occur only on the night side, especially in the early morning hours. Fields with scale sizes less than 15 km occur at all local time sectors.

In addition to the plots used in the investigation of the northern hemisphere events, two new plots were made to see if the events with large scale sizes and lower magnitudes could be sub-auroral electric fields (SAEFs, see e.g. [Marklund *et al.*, 1995b]) or fields directly connected to the aurora.

In Figure 3.12 these two plots are shown, the first showing the distribution of scale size over CGLat and the second showing the electric field strength distributed over CGLat. The spatially large field events occur at all latitudes between $-65°$ and $-77°$. The most equatorward event, with a magnitude of about 130 mV/m has a large scale size, and could be an example of a SAEF. The most poleward events have smaller scale sizes. Events with electric fields below 200 mV/m occur at all latitudes, and the proportions between events below and above 200 mV/m is approximately the same over the whole area.

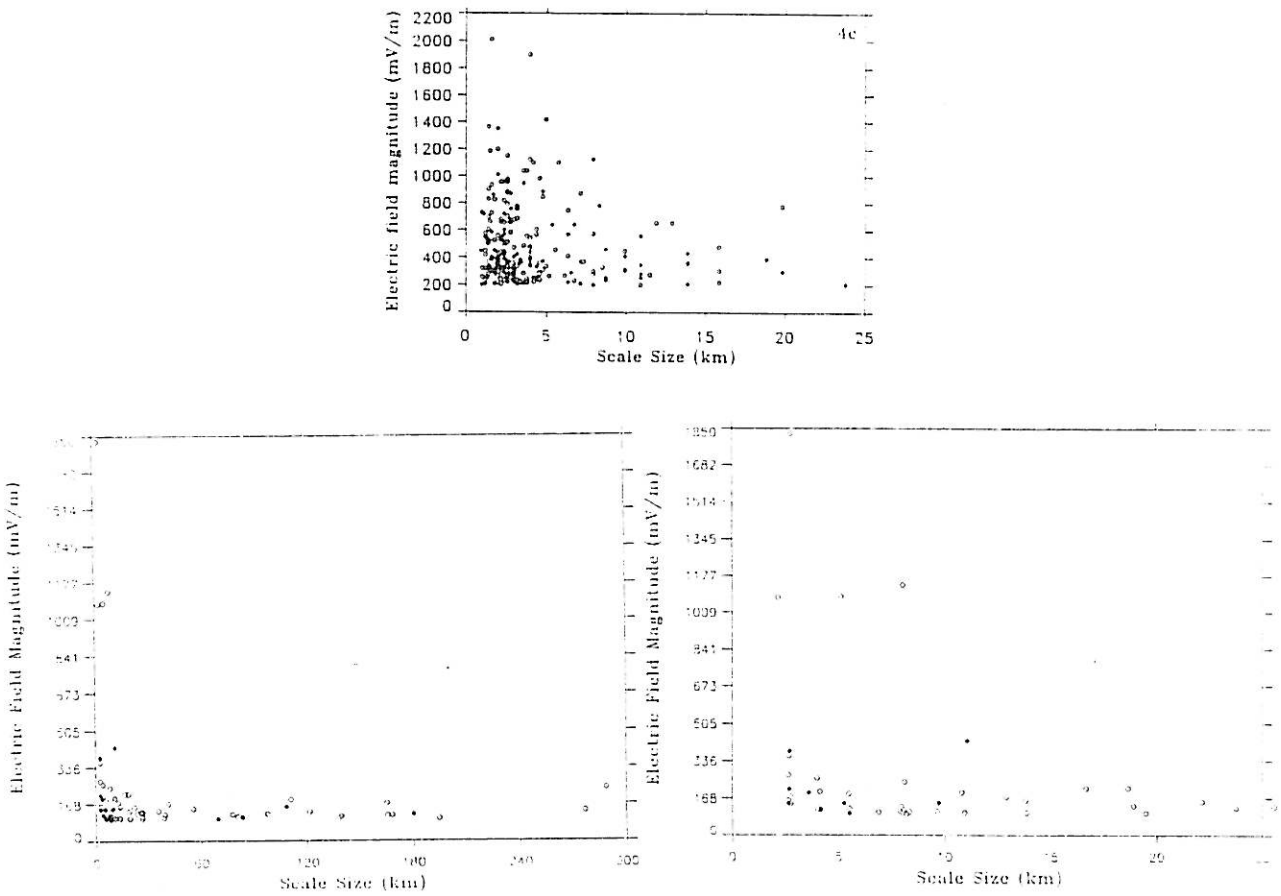

Figure 3.10: Electric field intensity vs scale size. *Top:* Higher altitude data. *Bottom left:* Lower altitude data, all events. *Bottom right:* Lower altitude data, events with scale size up to 25 km.

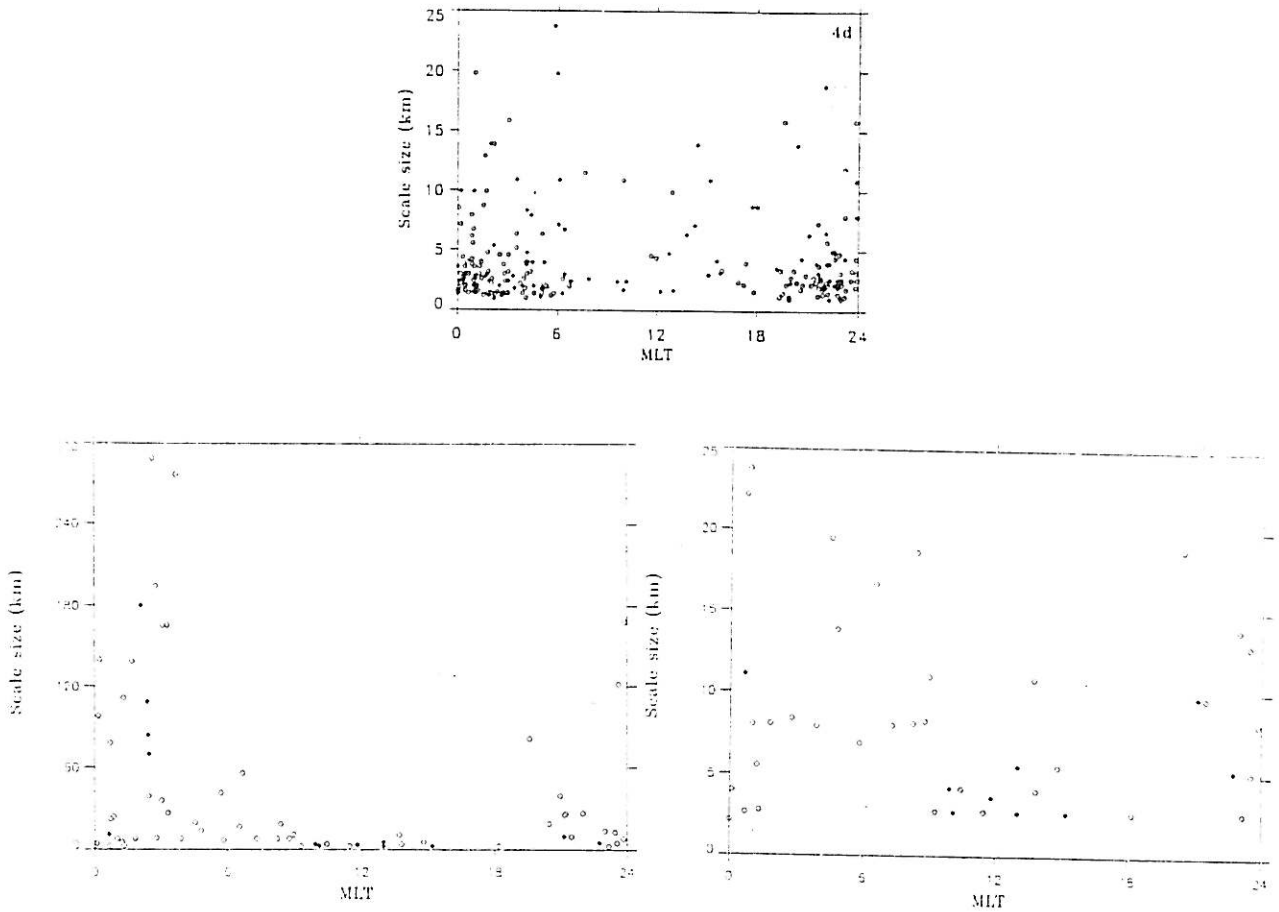

Figure 3.11: Scale size vs MLT. *Top:* Higher altitude data. *Bottom left:* Lower altitude data, all events. *Bottom right:* Lower altitude data, events with scale size up to 25 km.

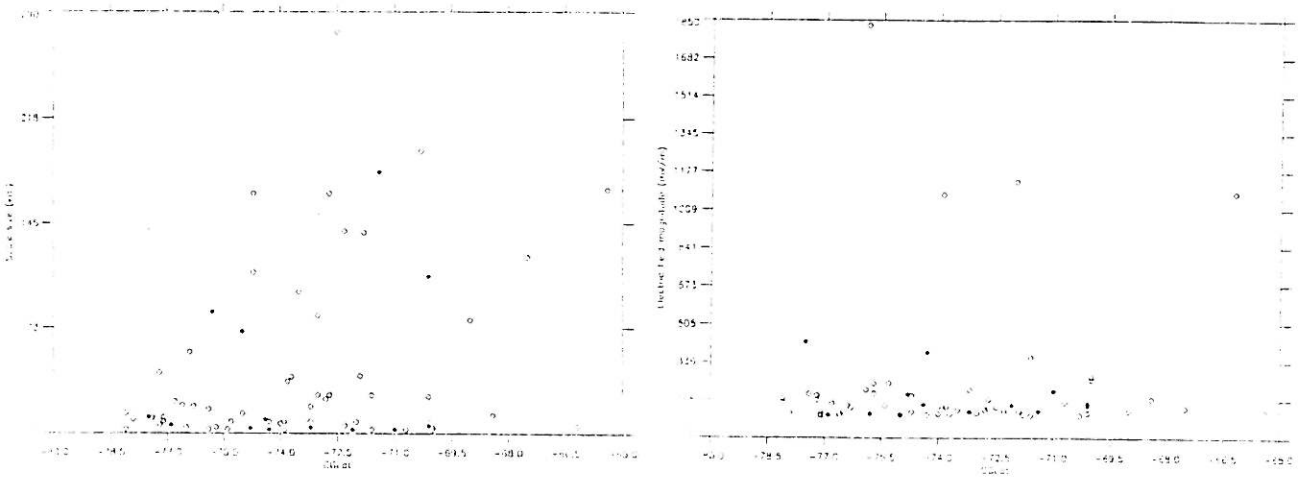

Figure 3.12: Southern hemisphere data. *Left:* Scale size vs magnetic latitude. *Right:* Electric field magnitude vs magnetic latitude.

3.4 Discussion

In the 1994 Freja electric field data from altitudes around 800 km, 69 events were found with electric field strengths exceeding 100 mV/m. The five strongest events, ranging from 427–1827 mV/m, was investigated in more detail. Two of these events were clearly seen to have a divergent structure. The statistical properties of the total collection of events were much alike what was found in the higher altitude investigation, though in general the events were fewer and less intense in the present study.

3.4.1 Interpretation of the Strongest Events

The event from orbit 9008, Figure 3.3 is one of the two with a clear divergent structure, which can be seen in the potential curve, having two potential maxima next to each other. The structure of the electric field is characterized by two very strong oppositely directed peaks, separated by 5–6 km where the field has a strong southward component. This indicates two possible configurations. One is that Freja passes obliquely from west to east through an east-west aligned dark filament, like those treated by Schoute-Vanneck *et al.* [1990]. The strong oppositely directed peaks should then correspond to when the satellite encounters the two ends of the dark filament. Another possible situation is that Freja passes through two adjacent black auroral curls. See Figure 3.13, which also shows a similar event from the higher altitude Freja investigation. The scale size of curls and separation fits with the event in orbit 9008.

The strongest field in orbit 9139, Figure 3.4, is also clearly diverging and is

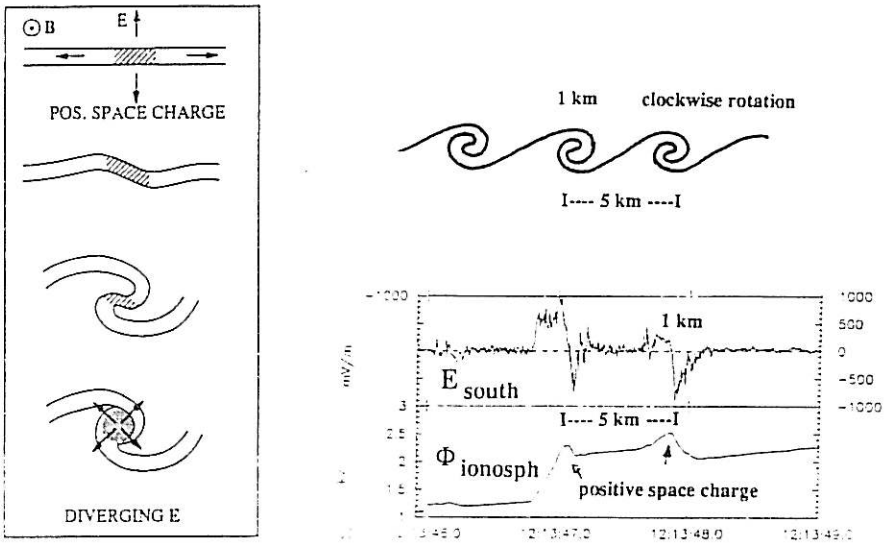

Figure 3.13: A schematic picture of how a black auroral band can go unstable forming black aurural curls, and an example of an event measured by Freja on the northern hemisphere which appears to be caused by such curls. (From Marklund *et al.* [1994])

surrounded by other large fluctuating fields. The strongest peak is rather wide, and in connection to the peak the potential curve indicates a local excess of positive charge. The maximum of that potential structure is located where the field shifts from having a strong westward component to having a very strong eastward component. Freja passed over this structure from northwest to southeast. A possible scenario is that Freja has passed across several auroral and black auroral bands. The strongest peak being directed eastward could correspond to the passing over a black auroral curl. Curls are typically associated with strong radial fields, which, depending of the location of crossing of the curl can show up in any direction, while bands are dominantly oriented in the east-west direction with associated fields mostly oriented in the north-south direction. In the north-south component of the electric field three peaks are seen separated by about 4–5 km. That could be an indication of a dark band going unstable and developing into black auroral curls.

The event in orbit 9176, Figure 3.5, is more difficult to interprete. Due to a large offset in the electric field data, it is impossible to figure out whether the field is diverging or converging, but there is a sharp gradient in the potential curve in connection to the event. There are no fluctuating fields around this event and it occurred at a comparably high altitude,1026 km above sea level. It is the event found at the highest altitude of this low altitude investigation. A possibility is that the field is associated with the acceleration region extending

to an unusually low altitude at this occasion. On the other hand the low latitude of this event, -66.2°, suggests that this might be a so called subauroral electric field, SAEF. However, SAEFs usually have scale sizes of the order 100 km and typically magnitudes less than 500 mV/m. It can not, however, be outruled that this may be an exceptionally intense SAEF event. In addition to the relatively low latitude of this event, the smooth behaviour of the field and lack of irregular fields — typical on auroral field lines — support such an interpretation.

The fields measured in orbit 9335, Figure 3.6, also suffer from a large offset making the calculated potential curve (or a vectorplot of the field) a useless tool for deciding whether the event is divergent or not. The size of this event is about 10 km, with a strong eastward component. The maximum of the electric field magnitude occurs close to the northeastern end of this structure, associated with a slight change in the potential curve. It is difficult to interpret this event in terms of possible auroral structures.

The strongest field, 1827 mV/m, is found on orbit 9348, Figure 3.7. The region in which this event occurs is one with rapidly changing fields with strong peaks in all directions. The most violent fluctuations go on for about one km before the satellite ceases to provide data. The 1827 mV/m peak — directed westward — is well within the region where the data are trustworthy. The satellite seems to pass through a turbulent area with several bands of aurora and black aurora. Before the maximum peak, the field changes from east through north to west. The potential shows several maxima and minima in the region, which reflects the possible mixture of auroral and black auroral structures.

3.4.2 The Overall Statistics

The characteristics and distribution of the collection of events from the northern and southern hemispheres, show large similarities, but there are important differences too. These imply certain similarities and differences in the physical situation at the two different altitudes investigated. The tresholds used to define an event were 200 mV/m and 100 mV/m in the higher and lower altitude investigations, respectively, and the number of events was much lower in the latter. This explains some of the differences in the output.

In both cases the events are mainly concentrated to the auroral region at each hemisphere. There is a tendency for events at more active times to be located more equatorward, which can be expected from the variation of the auroral oval with magnetic activity. The most intense fields occurred in the night to early morning local time sector. This MLT range is much more narrow in the southern hemisphere data set, which partly can be due to the lower number of events. Elsewhere, at other local times, the low altitude fields seldom exceeds 200 mV/m whereas the high altitude fields often reaches 500 mV/m or more. On the southern hemisphere but not on the northern, fields with scale sizes up to 290 km were found, depending on the different intensity treshold values used. Apart from this the intensity and MLT-distribution related to scale size were

similar in both investigations. The most intense fields tend to have smaller scale size and vice versa, implying an upper potential treshold for the field structures. Fields with scale sizes larger than 15 km occur only on the nightside.

All observations together, points out a possible potential structure. The same type of diverging strong fields that were found in the earlier investigation [Marklund *et al.*, 1994, 1995ab; Karlsson and Marklund, 1996] have been found in two cases in the present investigation. In the previous investigation such fields were found to be correlated to decreased conductivity and downward currents. If these fields more easily arise where the conductivity is locally lower this could explain why the most intense fields and the fields with the largest scale sizes occur on the night side where the conductivity in generally lower. The occurence rate as well as the intensity of the events is higher in the higher altitude investigation. This implies that there are parallel potential differences between the two heights. The earlier observations of precipitating ions and upward accelerated electrons indicate that there is a parallel potential drop with reversed polarity of that of the usual auroral acceleration.

3.5 Summary

Strong electric fields have previously been found in connection to the aurora e.g. by the DE satellites and by the Viking satellite. Those fields were mostly converging and found at acceleration region altitudes. With the Freja satellite, operating at lower altitudes and with better resolution than previous instruments, unexpectdedly strong diverging fields were found. A large number of events from the northern hemisphere, i.e. around 1700 km altitude, was collected and investigated. Comparing the electric field data to particle and magnetic field data, it was suggested that these intense diverging fields were connected to black auroral structures (bands,curls etc.) and arising to ensure current closure. To further check these ideas another investigation — the present — were made of intense field events on the southern hemisphere where Freja passed the auroral region at altitudes around 800 km. Strong diverging electric fields were found also at this altitude range, similar to those found in the northern hemisphere investigation. The distribution and statistical properties of the intense field events were also similar to what was found earlier. This together implies that the closure currents are necessary also at these lower altitudes. The main differences between the results of the two Freja electric field investigations, are the higher occurrence rate and the generally higher intensity of the events at the higher altitude. Assuming that the diverging fields also at the lower altitude are associated to upward accelerated electrons and downward accelerated ions, these differences imply that there is a parallel potential drop between the two altitude ranges investigated, with an opposite polarity to what is found in the auroral acceleration region. Noteworthy is also the more narrow MLT-range on the nightside southern hemisphere, in which the strongest fields occurred.

3.6 Acknowledgements

The author primarily wishes to acknowledge his tutor Tomas Karlsson, for firm guidance through this study, and Prof. Göran Marklund for useful comments on the work, and both for help in interpreting the results. Acknowledgements also to these and other people at the Alfvén Laboratory for other kinds of help, e.g. in form of literature and software. The author is a guest from Stockholm University, Department of Physics.

References

1. Bennet E. L., Temerin M., Mozer F. S., The Distribution of Auroral Electrostatic Shocks Below 8000-km Altitude, *Journal of Goephysical Research*, Vol. 88, No A9 7107-7120, 1983

2. Doe R. A., Vickrey J. F. and Mendillo M., Electrodynamic model for the formation of auroral ionospheric cavities, *Journal of Geophysical Research*, Vol 100, NoA6 9683-9696, 1995

3. Johnsson J. R. and Chang T., Nonlinear vortex structures with diverging electric fields and their relation to the black aurora, *Geophysical Research Letters*, Vol. 22, No 12, 1481-1484, 1995

4. Karlsson T. and Marklund G. T., A statistical study of intense low-altitude electric fields observed by Freja, *Geophysical Research Letters*, Vol 23, No 9, 1005-1008, 1996

5. Knecht D. J. and Shuman B. M., The Geomagnetic Field, in *Handbook of Geophysics and the Space Environment*, Jursa A. S. (editor), Air Force Geophysics Laboratory, US, 1985

6. Linqvist P.-A., Marklund G. T. and Blomberg L. G., Plasma Characteristics Determined by the Freja Electric Field Instrument,*Space Science Reviews* 70:593-602, 1994

7. Lyons L. R., Formation of Auroral Arcs Via Magnetosphere-Ionosphere Coupling, *Reviews of Geophysics*, 30, 93-112, 1992

8. Marklund G., Auroral Arc Classification Scheme Based on the Observed Arc-assosiated Electric Field Pattern, *Planet. Space Sci.*, Vol. 32, No. 2, 193-211, 1984

9. Marklund G., Blomberg L., Fälthammar C-G. and Lindqvist P-A., On intense diverging electric fields associated with black aurora, *Geophysical Research Letters*, Vol. 21, No. 17, 1859-1862, 1994

10. Marklund G., Karlsson T., Blomberg L. and P.-A. Lindqvist, Freja Observations of Intense Low-Altitude Electric Fields, in Proc. of *Cambridge Symposium/Workshop on Multiscale Phenomena in Space Plasmas*, 20-25 February 1995, Bermuda, 1995a

11. Marklund G., Blomberg L., Fälthammar C-G., Lindqvist P-A. and Eliasson L., On the occurrence and charachteristics of intense low-altitude electric fields observed by Freja, *Ann. Geophysicae* 13, 704-712, 1995b

12. Schoute-Vanneck H., Scourfield M. W. J. and Nielsen E., Drifting Black Aurorae?, *Journal of Geophysical Research*, Vol. 95, No A1, 241-246, 1990

13. Weimer D. R., Goertz C. K., Gurnett D. A., Maynard N. C. and Burch J. L., Auroral Zone Electric Fields From DE 1 and 2 at Magnetic Conjunctions, *Journal of Geophysical Research*, Vol. 90, No A8, 7479-7494, 1985

14. Weimer D. R. and Gurnett D. A., Large-Amplitude Auroral Electric Fields Measured With DE 1, *Journal of Goephysical Research*, Vol. 98, No A8, 13557-13564, 1993

Bibliography

1. André M. (editor) and the Freja Team, The Freja Scientific Satellite, *IRF Scientific Report 214*, Swedish institute of Space Physics, 1993

2. Burke W. J., Hardy D. A. and Vancour R. P., Magnetospheric and High Latitude Ionospheric Electrodynamits, in *Handbook of Geophysics and the Space Environment*, Jursa A. S. (editor), Air Force Geophysics Laboratory, US, 1985

3. Fälthammar C.-G., Rymdfysik, *Division of Plasma Physics, Alfvén Laboratory*, Sweden, 1990

4. Fälthammar C.-G., Plasmafysik, *Division of Plasma Physics, Alfvén Laboratory*, Sweden, 1993

5. Jacksson J. D., Classical Electrodynamics, *John Wiley & Son*, US, 1975

6. Whalen J. A., O'Neil R. R. and Picard R. H., The Aurora, in *Handbook of Geophysics and the Space Environment*, Jursa A. S. (editor), Air Force Geophysics Laboratory, US, 1985